E. Torroja bridge: Tailored experimental setup for SHM of a historical bridge with a reduced number of sensors.

Pablo Pachón[a,*], Rafael Castro[b], Enrique García[c], Víctor Compan[a], Esther Puertas[d]

[a]*Dept. of Continuum Mechanics, University of Seville, Avenida Reina Mercedes, 41012 Sevilla, Spain*
[b]*Dept. of Mechanics, University of Cordoba, Campus de Rabanales, 14071 Cordoba, Spain*
[c]*Department of Continuum Mechanics and Structural Analysis, Universidad de Sevilla, Camino de los Descubrimientos s/n, 41092 Seville, Spain*
[d]*Dept. of Mechanical Structures and Hydraulic Engineering, University of Granada, Avenida Fuentenueva, 18001 Granada, Spain*

Abstract

This paper presents a vibration-based Structural Health Monitoring of the historical bridge of Posadas (Córdoba, Spain), designed by the eminent engineer Eduardo Torroja in 1957. The importance of this study lies on the need for safeguarding this piece of cultural heritage. Due to the singularity of this historical construction, whose configuration of a concrete deck with inverted steel arch trusses can only be found in two other examples in Europe, in-service condition assessment is essential for its maintenance. It is well known that one of the main difficulties that need to be addressed in the structural analysis of this type of historical constructions is the high level of uncertainty derived from numerous parameters that characterize the structure. Aspects such as the material properties, the connections between structural parts or the construction process may cause important changes between the results obtained from a classical numerical analysis and those experimentally observed. Among non-destructive techniques, finite element modal updating allows for adjusting the numerical model on the basis of experimentally identified dynamic properties. Hence, the numerical finite element model can be tuned to accurately reproduce the current structural response of the structure. Once the numerical model is adequately tuned, it is possible to design experimental setups with a limited number of sensors and, therefore, to plan cost-efficient continuous monitoring. Hence, this paper presents the finite element modal updating of a three-dimensional finite element model of E. Torroja's bridge on the basis of a vibration-based monitoring and a genetic optimization algorithm. Afterward, an optimal sensor placement methodology has been utilized to design an experimental setup with a limited number of sensors. The results demonstrate that few sensors are needed to accurately assess the main resonant frequencies and mode shapes.

Keywords:
Ambient vibration, complex geometry, genetic algorithm, historic bridge, Operational modal analysis, optimal sensor placement

*Corresponding author.
Email address: ppachon@us.es (Pablo Pachón)

1. Introduction

Historical bridges constitute a key piece of the cultural heritage, inasmuch as they bear witness to the course of history and hold a social, cultural, and artistic value. The assessment of the health condition of these structures is thus absolutely crucial for the conservation of the historical patrimony. Structural Health Monitoring (SHM) encompasses the application of Non-Destructive Testing (NDT) and damage detection in order to extend the life-cycle of structures. In particular, Operational Modal Analysis (OMA) is considered one of the most adequate methods to assess the modal parameters of structures [1, 2]. OMA is performed under service conditions without the need for transferring artificial excitations, feature that results essential to dynamically characterize historical structures where the use of stronger external excitation, such as hammers or shakers, is often inadmissible. Nevertheless, OMA usually requires a high number of sensors to characterize the dynamic properties, fact that limits the scalability of OMA-based SHM to large scale structures and continuous monitoring. Given the high cost of such systems, it is usually difficult to persuade owners of the structures due to the low return of the investments.

The State of the Art contains many studies on finite element analysis and experimental investigation of historical bridges. Chiara Pepi et al. [3] studied the structural performance of a ancient bridge located in Todi (Umbria, Italy), through the integration of geometric survey, dynamic testing and numerical modeling. Another noticeable work was done by B. Conde et al. [4] concerning the ambient vibration testing of the Vilanova Bridge, a masonry structure located in Galicia (Spain), whose origin dates back to the 13th-14th centuries. They presented a multidisciplinary approach for the structural assessment of masonry arch bridges by using non-destructive testing techniques and three-dimensional numerical modelling. Gentile and Saisi [5] conducted the dynamic characterization of two historic structures: The Collegiata of San Vittore bell tower (Arcisate, Italy) and the San Michele bridge (Milan, Italy), a arch bridge built in 1889. Those authors studied the variation of the dynamic characteristics of the bridge under different traffic conditions. Finally, it is worth noting the work done by Altunisik et al. [6] on a mid-nineteenth century bridge in Turkey, the Mikron arch. In that study, they presented the Finite Element Modelling (FEM), the vibration-based operational modal analysis, and the finite element model updating of this restored historic arch bridge. However, despite the great effort put into implementing these techniques to the conservation of historical constructions, the elevated costs of these systems still remain an important drawback.

This paper aims at presenting a methodology to tailor monitoring systems with a small number of sensors in order to continuously assess the structural health of the E. Torroja bridge. This bridge was constructed in 1951 on the Guadalquivir river by the renowned civil engineer Eduardo Torroja (Fig. 1). The cultural and historical importance of this bridge justifies the development of a long-term SHM system. For this purpose, the most suitable monitoring locations are defined by means of Optimal Sensor Placement (OSP) algorithms. OSP algorithms are based on a numerical model of the structure and maximize the modal information with a reduced number of degrees of freedom, that is to say, a limited number of sensors. Hence, it is crucial to count on an accurate numerical model capable of correctly determining the position of the sensors. To this end, a preliminary ambient-vibration test was first conducted to assess the vibrational properties of the structure and serve as basis for the updating of the numerical model. The discrepancies between the theoretical and the experimental results were minimized by updating different variables in the model such as the boundary conditions, the stiffness and connectivity of the structural elements, as well as the material properties. Once the numerical model was tuned and could correctly reproduce the

dynamic properties of the structure, the optimal locations of a long-term monitoring system with a reduced number of sensors were determined by an OSP algorithm.

Figure 1: Eduardo Torroja Bridge in Posadas, Córdoba (Spain).

The paper is organized as follows: Section 2 presents a brief historical evolution of the bridge together with its geometric configuration. Section 3 introduces the numerical model of the bridge used during the development of the present study. Section 4 presents the dynamic characterization of the bridge by means of an experimental OMA campaign. Section 5 is devoted to discuss the updating process of the FE model. Section 6 introduces the optimal sensor placement technique followed to organize the structural health monitoring. Finally, Section 6 draws the main conclusions of this study.

2. E. Torroja Bridge: Construction and evolution.

D. Eduardo Torroja Miret (1899-1961) is considered one of the major figures in the Spanish civil engineering, with a fundamental contribution to the design of light concrete shell structures. In his book *"Razón y Ser de tipos estructurales"* [7], Torroja explains his oeuvre as a quest for structural truth, a concept through which beauty lies on rationality and not on artificial ornamentation. With this in mind, Torroja developed new ways of looking at structures as well as to increase their load bearing capacity, that is, to increase their strength without compromising aesthetics. Torroja showed an interest in forms of art that are present within most of his structures which often incorporated his vision. There are numerous historical bridges designed by this eminent engineer, such as the Muga Bridge (Fig. 2a) or the Pedrido Bridge (Fig. 2b).

(a) (b)

Figure 2: Views of (a) Muga Bridge, 1939 (Girona, Spain), and (b) Tordera Bridge, 1939 (Barcelona, Spain).

After the Spanish civil war, E. Torroja was commissioned to substitute the bridge over the Guadalquivir River in Posadas (Córdoba, Spain) which had been seriously damaged in the conflict. The original structure, consisting of reinforced concrete arches, was replaced by five steel-concrete composite spans of 43 m (Fig. 3). The new solution was defined by a compressive reinforced concrete deck 7 m width bonded to two steel arches, both defined by an upper horizontal beam and a parabolic arch with maximum rise of 6 m. Figure 4 shows two photographs of the original bridge under construction.

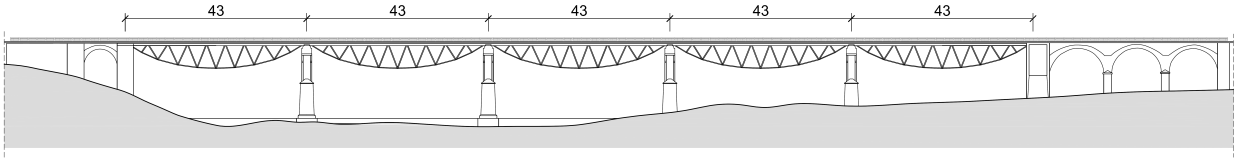

Figure 3: Front view of E. Torroja Bridge (Units in meters)

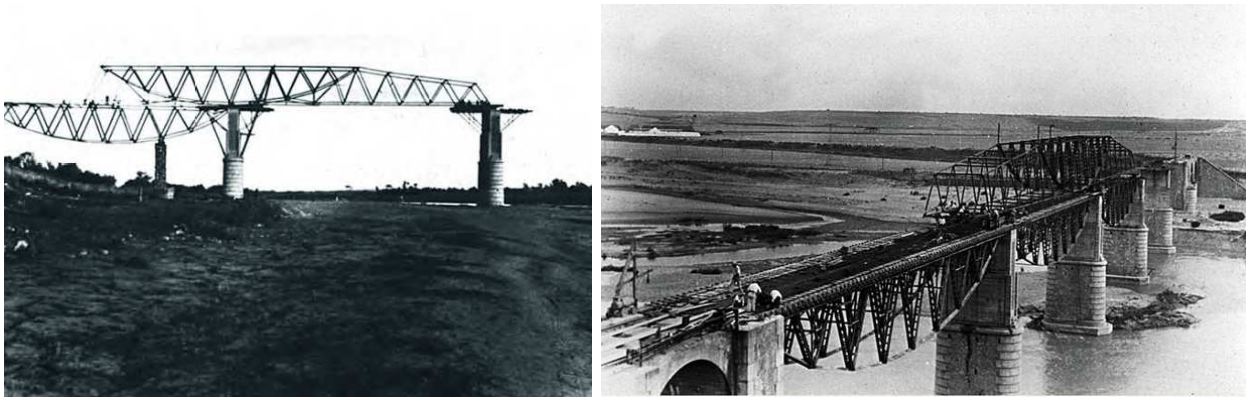

Figure 4: Photographs of the original bridge under construction.

In 1983, some new repairs were conducted in the deck such as new dilatation joints, injections,

and repairs on the piles' and abutments' walls. In addition, some damaged steel components were replaced and, eventually, the metallic structure and handrails were repainted. Nonetheless, the structural typology was kept unaltered (see Fig. 5).

Figure 5: Photographs of the original bridge in service.

In 1991, E. Torroja's grandson, Antonio Torroja, was entrusted to carry out an extension of the deck width from 6.5 m (Fig. 6 (a)) to 11 m (Fig. 6 (b)). To this end, two new arches were added and attached to the original ones by a tubular truss structure. The original deck had to be completely removed because new upper reinforcements were needed to bear the transverse negative moments (Fig. 7).

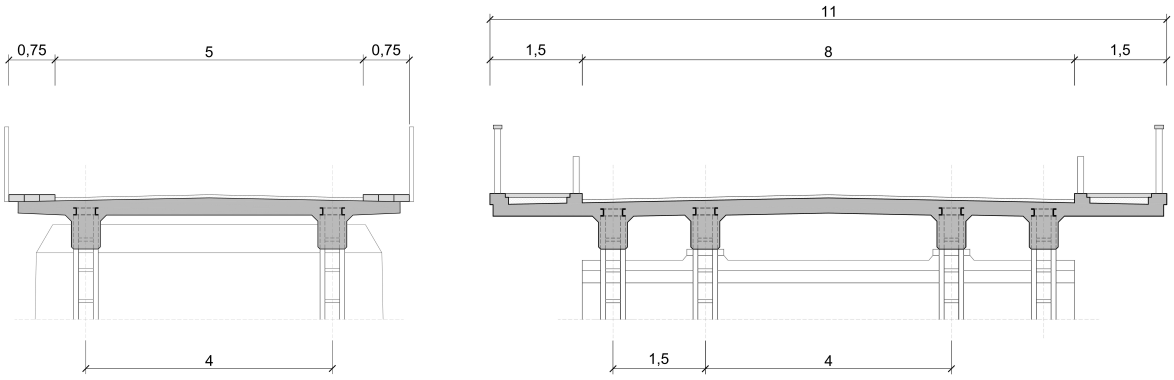

(a) Original cross section.

(b) Re-designed cross section.

Figure 6: Cross sections of the bridge (m).

(a) (b)

Figure 7: Views of (a) initial and (b) final operations of deck's width increment (1992).

It should be noted that all the modifications experienced by the structure entail a high level of uncertainty, affecting both the material properties and the structural behavior. Moreover, due to the singular geometry that characterizes the bridge, the metallic part of the structure is not physically accessible (Fig. 8), so the experimental modal characterization of the bridge must be carried out on the road. In this sense, the numerical model analysis is presented as a fundamental tool to evaluate the current state of conservation of the bridge in general and the structural steel part in particular.

Figure 8: Views of the Current Bridge in service.

3. Finite element modal analysis

3.1. Structural evolution of the bridge.

As previously indicated, the bridge experienced important modifications since its construction. Some of original elements were preserved, whilst some others were later incorporated. Hence, it is evident that there exists a high level of uncertainty stemming from differential aging processes. In order to shed some light on the evolution of the structural behavior of the bridge, the authors of this paper carried out a preliminary research that was presented in the *International Modal*

Analysis Conference (IMAC 2015) [8]. In that study, both the original and the current designs of the bridge (see Fig. 6) were simulated by preliminary FEMs. Then, a comparison of both models in terms of their dynamic properties was made in order to aid in the understanding of the structural evolution. Beam elements were used for all the components except for the deck for which thick shell elements were utilized. Finally, the resonant frequencies of both structures were computed by modal analysis and it was observed that only small differences are found in the first five modes. This fact indicates that, despite the considerable modifications experienced by the structure, the dynamic behavior of the bridge was not significantly altered. Therefore, it was concluded that the increases in the stiffness of the bridge was accompanied by a similar increase in its mass, where the change of weight of steel per area of deck from 66.22 to 79.33 kg/m^2 is indicative of this conclusion. It was also concluded that, since the dynamic characteristics had not been apparently altered, the different operations conducted in the bridge may have introduced uncertainties stemming from differential aging processes.

3.2. FEM of the current bridge

In order to incorporate all the geometrical details of the structure, a sophisticated model is developed. Due to the large size of the E. Torrojas bridge including five simply supported spans, the FE models of the overall bridge would result in a large computational cost. Moreover, each span of the bridge behaves as an independent part to the others, since there is no structural connection between them. Therefore, a simplified model of a single span was applied, as is also usual in the study of this type of bridge. Only shell elements are defined in such a way that the connection between the steel arches and the concrete desk can be accurately simulated (Fig. 9). The horizontal braces are built-up sections with UP120 profiles and batten plates of dimensions 400x50x8 mm every 50cm. The arches are also built-up sections with IP200 profiles and batten plates of dimensions 210x50x8 mm every 50cm. Due to the complexity in the geometry of the profiles and the joints, 3-node-shell elements are used for all the steel members. With regard to the concrete slab, regular 4-node-shell rectangular elements are defined. Overall, the complete model has 374.928 elements, 388.679 nodes and 2.332.074 degrees of freedom. Boundary conditions are defined as constrained displacements and free rotations, as can be observed in the details of the figure 9. Table 1 summarizes the material properties used in the modeling. All the values selected to define each material are usual in the design of this type of structure, with the exception of steel density, whose value increases by 1.9 % taking as reference its standard value. This decision is taken to consider all those factors that have not been taken into account when defining the numerical model, such as welds, bolts and other auxiliary elements. The weight of the battens and the road are also included in terms of added mass.

Property	Unit	Value
Mass of security barriers	kg/m	14.66
Mass of asphalt	kg/m^2	110
Young's modulus of concrete slab	MPa	30000
Poisson's ratio of concrete slab	-	0.2
Density of concrete slab	kg/m^3	2500
Young's modulus of steel	MPa	210000
Poisson's ratio of steel	-	0.3
Density of steel	kg/m^3	8000

Table 1: Material properties used in the FEM.

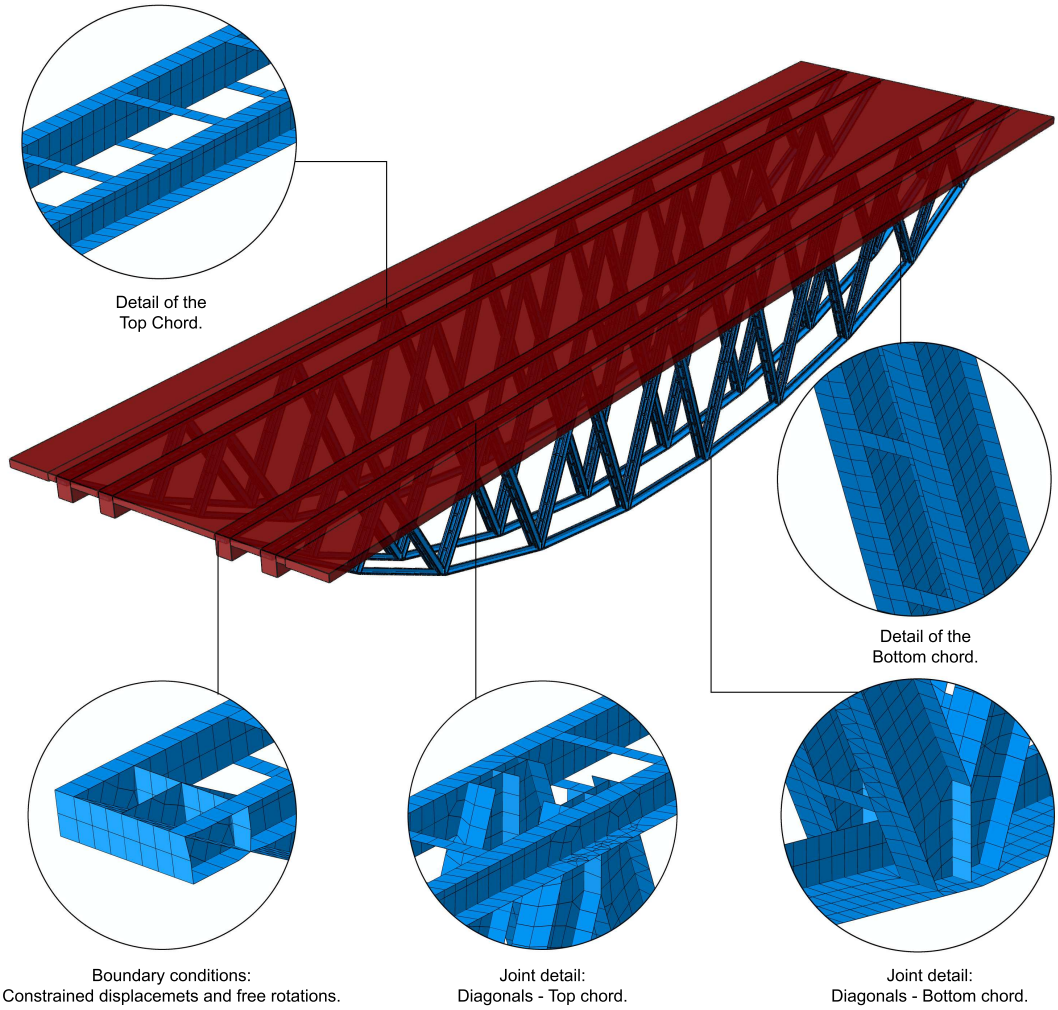

Figure 9: FEM of the current state of the E. Torroja's bridge.

Afterward, the modal properties of the structure are computed by a modal analysis in Abaqus CAE [9]. The first eight mode shapes are shown in Fig. 3.2.

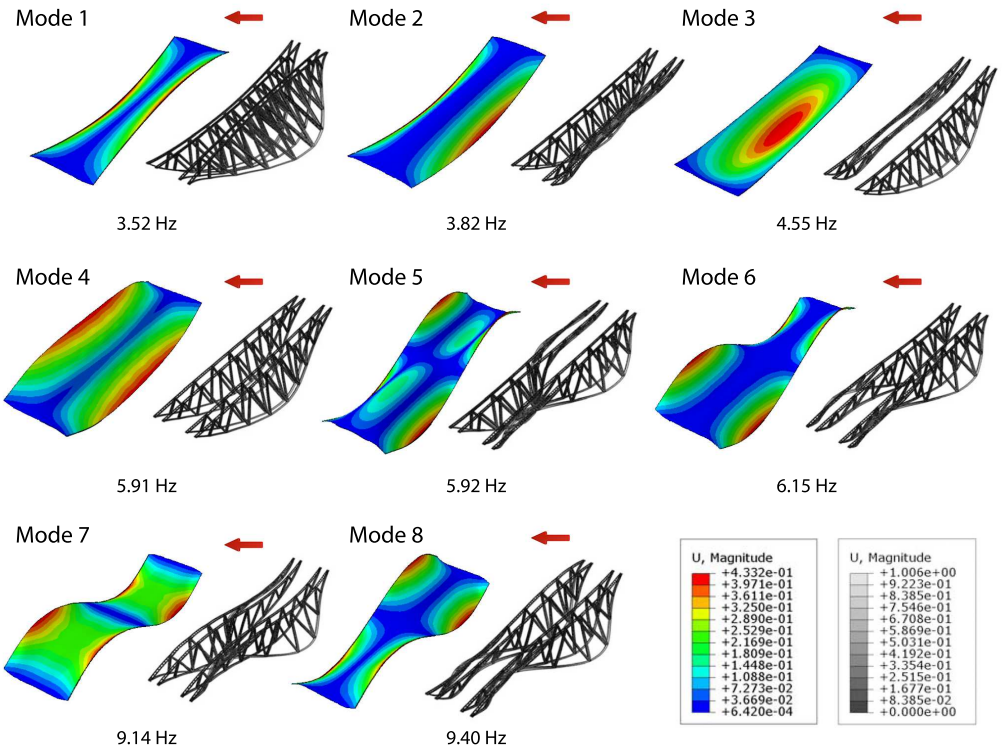

Figure 10: First eight numerical eigenmodes computed by the FEM of E. Torroja bridge.

4. Ambient vibration tests and Operational Modal Analysis technique

The dynamic testing of the structure can provide an accurate prediction of its global modal parameters. In view of the mode shapes in Fig. 3.2, it is clear that the structure has a narrow band of low natural frequencies and highly coupled, what makes the dynamic features of the structure quite complex. For this reason, an extensive ambient vibration campaign on the E. Torroja Bridge was conducted on 14 of March 2017 to ensure an efficient identification of the modal properties.

4.1. Ambient vibration tests

The position of the reference acceleration sensor was chosen according the results provided by the numerical model [10]. The sensor configuration is plotted in Figure 4.1. The set-up consists of a total of 36 measuring points. All the measuring points were set in the three principal directions with the aim of identifying the vibration modes in the lateral, longitudinal and vertical directions of the bridge. Since one of the accelerometers (placed at point 6, Fig. 4.1) were kept fixed as a reference, twelve set-ups were performed to complete the experimental campaign. In each one of these set-ups, a sampling time of 10 min and a sampling rate of 100 Hz were selected, taking into account the empirical rule proposed by J. Rodrigues in his Phd Thesis [11]. These assumptions ensure that frequencies from 1 to 50 Hz would be properly recorded.

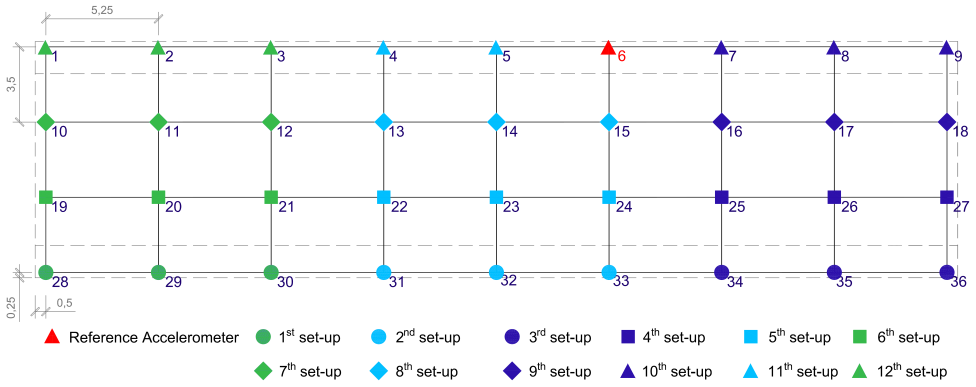

Figure 11: Plan view of the accelerometer locations (Reference accelerometer in red).

The equipment used for these tests included five self-contained recorder instruments manufactured by the company GeoSIG Measuring Systems. These instruments have three internal sensors, anti aliasing filters, a bandwidth ranging from 0.01 to 250 Hz, a dynamic range of 146 dB, a sensitivity of 10 V/g, and 4.70 kg of weight (model GMSplus) (Fig. 12).

Figure 12: Self-contained recorder instrument (GMSplus).

The same conditions of temperature and humidity were taken into account during the whole test in order to avoid variations in the modal parameters [12]. In addition, the modal excitation of the bridge was always caused by environmental loads, such as wind or traffic. (Fig. 4.1).

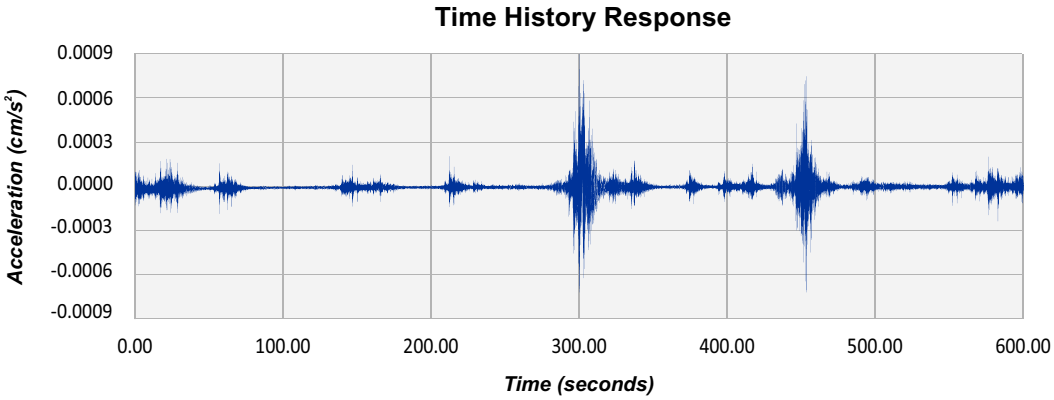

Figure 13: Time history response (ambient excitation registered for accelerometer number two, 4th set-up).

4.2. Operational Modal Analysis

The Artemis Software [13] was used to analyze the data obtained during the experimental campaign. The Enhanced Frequency Domain Decomposition (EFDD) technique [14, 15] and the Stochastic Subspace Identification (SSI) method [16, 17] were the two different identification methods used to obtain the modal parameters of the bridge (Fig. 14). In order to perform a more accurate analysis some decisions were taken during signal processing. A decimation factor of 5 was applied to the signal in order to take into consideration that the expected natural frequencies are below 10 Hz, as can be observed in Figure 10. In addition, the resolution of the spectral density estimation was defined as 1024, resulting a frequency line spacing of 0.005 Hz. Harmonic detection algorithms were also applied in order to check all frequencies in the spectrum.

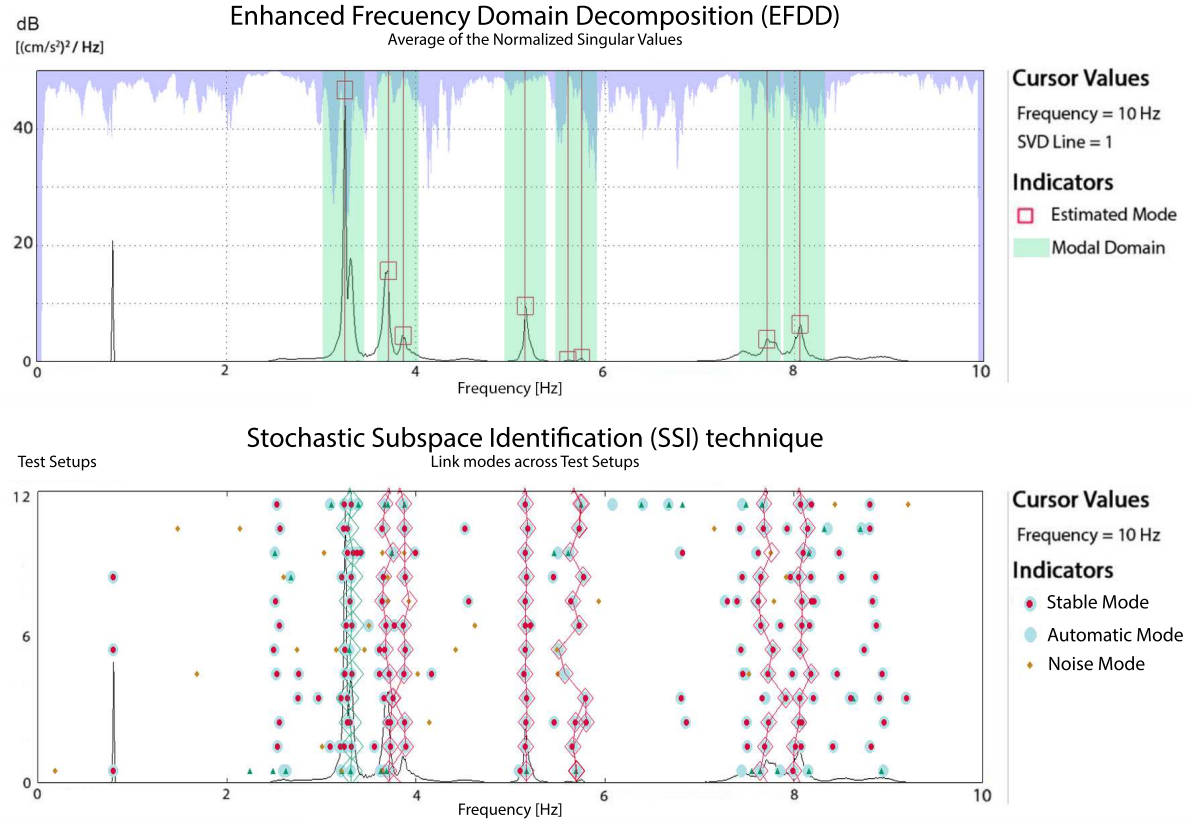

Figure 14: Identification of the resonant frequencies by EFDD and SSI techniques.

In order to validate the identified modal parameters, the Modal Assurance Criterion (MAC) [18] was applied. Given two mode shapes φ_j and φ_k, their MAC value responds to:

$$\mathbf{MAC}_{j,k} = \frac{(\boldsymbol{\varphi}_j^T \cdot \boldsymbol{\varphi}_k)^2}{(\boldsymbol{\varphi}_j^T \cdot \boldsymbol{\varphi}_j) \cdot (\boldsymbol{\varphi}_k^T \cdot \boldsymbol{\varphi}_k)} \tag{1}$$

where T designates transpose. When the MAC value is higher than 0.80, a good correlation between the two modes is considered [18]. Finally, Table 2 presents the obtained results, including the standard deviation of modal frequencies and damping ratios.

Mode No.	SSI				EFDD				MAC
	f (Hz)	std(f)	ξ (%)	std(ξ)	f (Hz)	std(f)	ξ (%)	std(ξ)	
1	3.28	0.02	0.85	0.40	3.31	0.01	1.46	0.66	0.92
2	3.68	0.07	0.79	0.46	3.72	0.03	2.14	1.17	0.94
3	3.80	0.04	0.78	0.31	3.84	0.07	1.60	1.01	0.82
4	5.14	0.01	0.60	0.17	5.16	0.01	0.63	0.22	0.98
5	5.61	0.10	0.38	0.27	5.68	0.09	2.78	1.16	0.81
6	5.64	0.05	0.41	0.26	5.69	0.07	2.01	1.22	0.80
7	7.79	0.05	0.58	0.31	7.68	0.14	1.70	1.06	0.86
8	8.02	0.02	0.49	0.27	8.07	0.05	0.84	0.39	0.84

Table 2: OMA results: natural frequencies (f), damping ratios (ξ) and standard deviation (std).

As can be observed in Table 2, it was possible to identify the first eight vibration modes in a frequency range up to 10 Hz. The differences between the frequencies were always lower than 1.5%, taking the results of the SSI method as reference. The results for the damping ratio show an higher variability, with average modal damping ratios of 0.61% and 1.64% for SSI and EFDD techniques, respectively. These high differences are typically found in practice what indicates that different and higher levels of excitation are required to accurately capture the damping ratios [19]. The damping values obtained by the EFDD method are even less reliable than those obtained by the SSI method, as can be deduced from the high standard deviation values obtained. With regard to the mode shapes, MAC indicates a good correlation between both methods with values higher than 0.80. The first and the fourth modes are torsional modes, while the other modes correspond to bending modes of the bridge (Fig. 4.2).

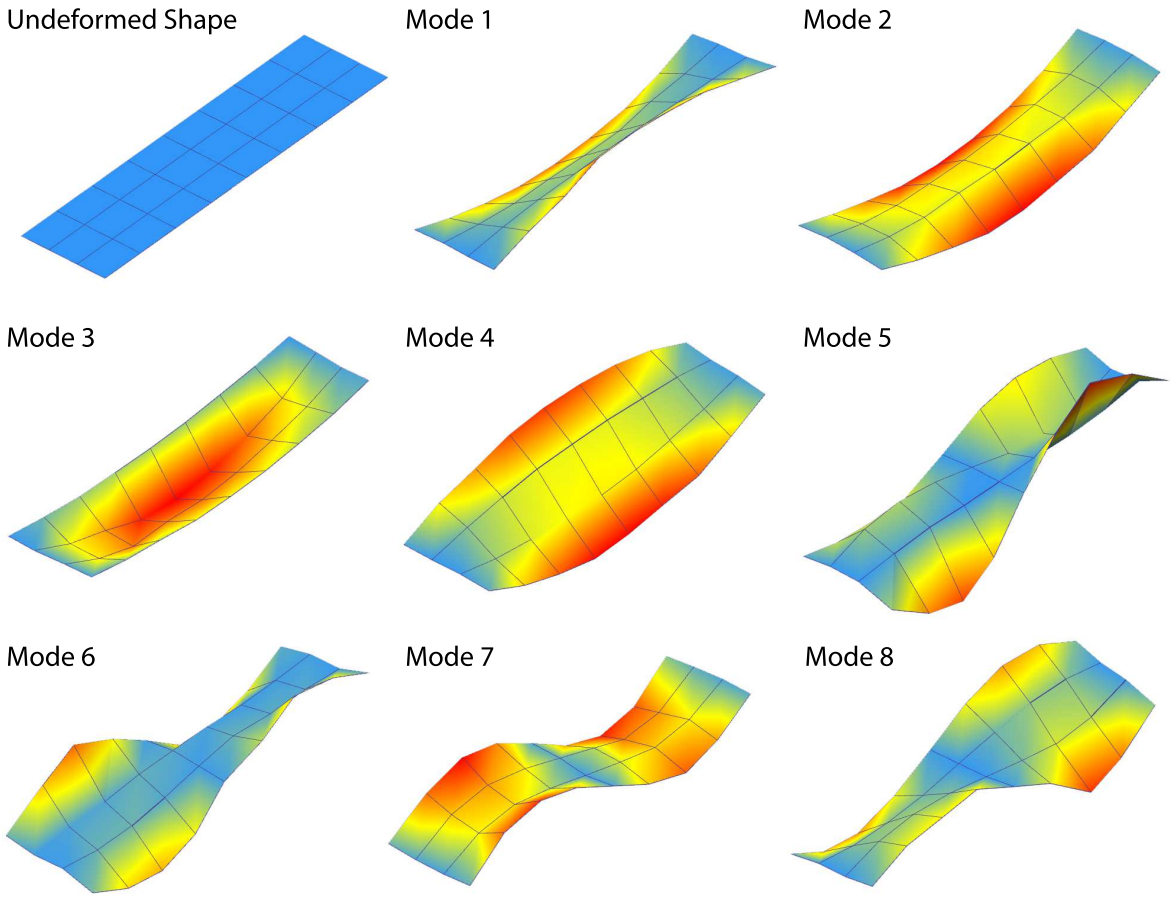

Figure 15: Experimental natural vibration modes.

5. Model updating

Based on the results obtained from the dynamic characterization of the bridge, the numerical model was updated to prepare the structural health monitoring by using optimal sensor placement techniques. Standard FE models of this kind of buildings usually include uncertainties derived from unknown material properties, existing damage, complex internal composition of structural elements and modelling approximations. Therefore, the calibration of the model with the aid of experimental information becomes necessary to appropriately model the actual structural behavior.

Following the same procedure as in previous research [20], the FE model updating was performed by means of iterative methods [21], in which the user introduces changes directly on some of the physical parameters that define the structure. With this aim, a sensitivity study was carried out to detect those structural parameters that have a greater influence on its dynamic behavior. These parameters were the Young's modulus (E_c) and the density of the concrete desk (ρ_c).

Once the updating parameters of the numerical model were selected, and considering the good quality of the experimental measurements, the three first identified modes were selected for the updating process. Taking into account the values of the natural frequencies and the modal coordinates, a total of 111 residual components were adjusted and minimized throughout the model

updating. In order to consider the greater credibility of the identified frequencies with respect to the modal displacements, for the natural frequencies the value of the variable was defined as $w_f = 1.00$, whilst for the modal coordinates this value was defined as $w_s = 0.05$. Finally, the FEM updating was performed via a genetic algorithm in Matlab [22], according to the objective function defined by the relative differences between the experimental and numerical modal parameters. This function is usually formulated as a least square problem:

$$l(\theta) = \frac{1}{2}\sum_{j=1}^{m} w_j [z_{NUM,j}(\theta) - z_{EXP,j}]^2 = \frac{1}{2}\sum_{j=1}^{m} w_j r_j(\theta)^2 \tag{2}$$

where $z_{NUM,j}(\theta)$ are the values related to the physical parameters of the numerical model, θ (modulus of elasticity, density...), while the variables $z_{EXP,j}$ are the same magnitudes obtained from the experimental campaign. The differences between these variables are set as residues, $r_j(\theta)$. It must be noted that the number of residues, $m = m_f + m_s$ (with m_f being the number of natural frequencies considered and m_s the number of the coordinates of the considered vibration modes), is greater than the number of adjusted variables, θ. Weight factors w_j are the values established for each residue (from natural frequencies and vibration modes coordinates), which are applied in the equation above according to the following expressions:

$$r_{f,j}(\theta) = \frac{f_{NUM,j}(\theta) - f_{EXP,j}}{f_{EXP,j}}, j = 1, 2, ..., m_f \tag{3}$$

where $f_{NUM,j}(\theta)$ and $f_{EXP,j}$ are the values of the obtained frequencies from the numerical and experimental model. In a similar way, the residues in terms of mode shapes correspondingly write:

$$r_{s,j}(\theta) = \frac{\varphi^l_{NUM,j}(\theta)}{\varphi^r_{NUM,j}(\theta)} - \frac{\varphi^l_{EXP,j}}{\varphi^r_{EXP,j}}, j = 1, 2, ..., m_s \tag{4}$$

where $\varphi^l_{NUM,j}(\theta)$ and $\varphi^r_{NUM,j}(\theta)$ are the selected and reference component of the numerical mode j, while $\varphi^l_{EXP,j}$ and $\varphi^r_{EXP.j}$ are the same magnitudes obtained from experimental mode j. Then, in order to minimize this objective function, genetic algorithms are applied.

Figure 16 illustrates the updating process, showing its importance for obtaining numerical models that replicate the real response of the structures. Based on the properties of the initial FEM, and establishing a range of values for each updating parameter (Table 3) and the updating objective, the calibration process started. In each iteration, a population of 1000 vectors was considered by using the genetic algorithm principles (as implemented in Matlab software), and the objective function in Eq. (2) was minimized. Such calibration process terminated when the difference between the mean value (blue points in Fig. 16) and the best value (green points in Fig. 16) of the population was less than $1\text{x}10^{-3}$.

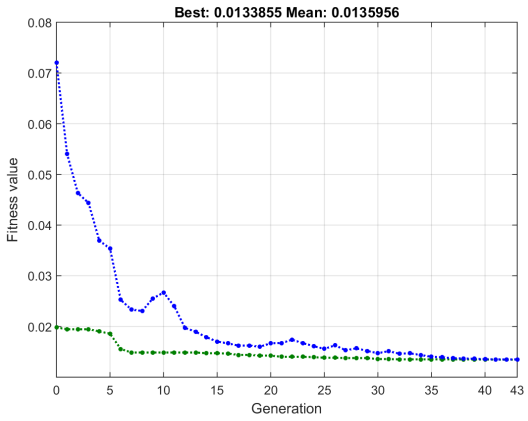

Figure 16: Genetic algorithm. Fitness value $l(\theta)$ versus Generation. Blue points: Mean values of the objective function of all the population of the corresponding generation. Green point: Best values result of an individual of the population.

Table 3 presents the summary of the updating process, highlighting the large differences the great differences that exist between the updated and initial parameters.

Parameter	Initial value	Interval		Updated value
		Lower	Upper	
E_c (MPa)	25000	20000	30000	27790.51
ρ_c (kg/m^3)	2500	2000	4000	3774.71

Table 3: Summary of updated parameters of the FEM by a genetic algorithm.

The results obtained from the updating process were also evaluated through the comparison of the experimental and numerical modes. To this end, a good correlation between two modes is considered when the relative difference between their frequencies $\Delta f_j = r_{fs,j} \cdot 100\% \leq 5\%$, and the $MAC_{NUMj,EXPj}$ value is greater than 0.85. In this sense, Table 4 confirms not only the high correspondence of the updated modes, but also the rest have been adjusted to the experimental results (relative difference between frequencies lower than 4% and MAC values higher than 0.80).

Mode No.	f_{SSI} (Hz)	$f_{(\text{prel. FEM})}$ (Hz)	$f_{(\text{FEM updated})}$ (Hz)	$MAC_{(\text{SSI-FEM upd.})}$
1	3.28	3.52 (7.31%)	3.26 (0.60%)	0.96
2	3.68	3.82 (3.81%)	3.67 (0.27%)	0.93
3	3.80	4.55 (19.73%)	3.90 (2.63%)	0.83
4	5.14	5.91 (14.98%)	5.26 (2.33%)	0.94
5	5.61	5.92 (5.52%)	5.77 (2.85%)	0.88
6	5.64	6.15 (9.04%)	5.82 (3.19%)	0.82
7	7.79	9.14 (16.81%)	7.83 (0.51%)	0.92
8	8.02	9.40 (17.20%)	8.08 (0.74%)	0.84

*The percentages in parenthesis correspond to the relative differences between frequencies.

Table 4: Comparison of natural frequency values and vibration modes experimentally (f_{SSI}) and analytically ($f_{(\text{prel. FEM})}$) obtained.

In Table 4, it can also be observed that the results of the mode shapes (Fig. 3.2) are also of high quality since in all the cases the MAC values are relatively close to 1.0 (and always higher than 0.80).

6. Optimal sensor placement

This section aims at tailoring a monitoring setup for the E. Torroja's bridge with a reduced number of sensors apt for cost-efficient long term SHM. For this purpose, different OSP methodologies have been proposed in the literature [23, 24]. In this work, the Effective Independence Method (EFI) [25] has been utilized. The EFI method searches the optimal Degrees Of Freedom (DOFs) that maximize the linear independence of the numerical modes of vibration. Since this methodology is model-based, the previous model updating process is crucial in order to ensure the accuracy of the optimal locations.

Firstly, a reduced modal matrix is computed by retaining only those modes of interest in the monitoring. Afterward, all those DOFs that cannot be physically monitored, such as rotational or inaccessible DOFs, are deleted. The Fisher Information Matrix, **FIM**, of the target modal matrix $\overline{\boldsymbol{\varphi}}$ reads:

$$\mathbf{FIM} = \overline{\boldsymbol{\varphi}}^T \overline{\boldsymbol{\varphi}} \tag{5}$$

FIM is symmetric and positive semi-definite. Hence, the EFI method selects the optimal DOFs that maximize the determinant of **FIM**. To this end, the contribution of the different DOFs to the linear independence of the target mode shapes can be computed by means of the orthogonal projection matrix, **E**, as:

$$\mathbf{E} = \overline{\boldsymbol{\varphi}}\, \mathbf{FIM}^{-1}\, \overline{\boldsymbol{\varphi}}^T \tag{6}$$

The elements of the diagonal of **E** represents the relative contribution of the i^{th} DOF to the rank of **FIM**. This property is due to the idempotence of **E** through which its rank equals the sum of the diagonal terms. The EFI method is thus defined in an iterative way eliminating those DOFs whose contribution to the rank of the **FIM** is minimal, that is, the lowest diagonal terms of

E. An extensive explanation of this methodology can be found in [23], and that can be concisely summarized as follows:

1. The rows of the modal matrix which correspond to DOFs which cannot be physically measured are omitted.
2. The DOFs which are required a priori for engineering reasons should be retained.
3. Target modes are selected. Only the columns from the modal matrix that correspond to those target modes are retained.
4. The orthogonal projection matrix **E** is computed and the DOF that yields the lowest diagonal term in **E** is eliminated.
5. This process is repeated until the number of DOFs that remain are equal to the desired number of sensors.
6. At every step the **FIM** matrix determinant determines the evolution of the process. Usually it is represented as the percentage of the initial value.

This procedure for the EFI optimal sensor placement method produces a sub-optimal solution in an iterative way. Thus, one hundred and five candidate nodes were selected, all of them located on the lower surface of the deck in order not to impede the normal operation of the bridge (Fig. 17). The testing process was performed taking into account that only four triaxial accelerometers are available to plan the structural health monitoring of the bridge. In this way, a total of four nodes would be selected as measuring points (blue points, Fig. 17).

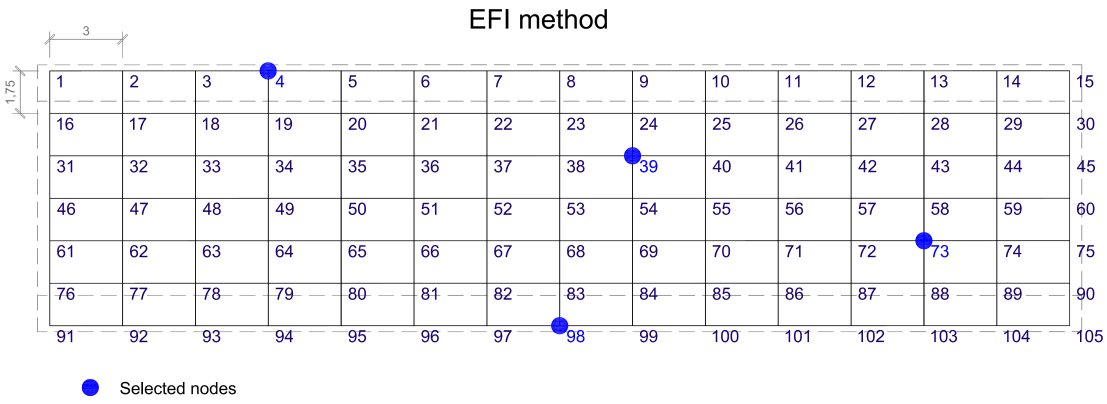

Figure 17: Optimal sensor placement locations (plan view of the bridge). Selected nodes in blue.

Based on the data obtained by the OSP method, Table 5 shows the comparison between the frequencies obtained from the general experimental campaign and those that would be obtained from the four selected points.

Mode No.	General campaign		OSP method	
	f_{SSI} (Hz)	f_{EFDD} (Hz)	f_{SSI} (Hz)	f_{EFDD} (Hz)
1	3.28	3.31	3.24 (1.21%)	3.28 (0.90%)
2	3.68	3.72	3.66 (0.54%)	3.71 (0.26%)
3	3.80	3.84	3.86 (1.57%)	3.87 (0.25%)
4	5.14	5.16	5.16 (0.38%)	5.15 (0.19%)
5	5.61	5.68	5.67 (1.06%)	5.61 (1.23%)
6	5.64	5.69	5.69 (0.88%)	5.67 (0.35%)
7	7.79	7.68	7.71 (1.02%)	7.71 (0.39%)
8	8.02	8.07	8.05 (0.37%)	8.04 (0.37%)

*The percentages in parenthesis correspond to the relative differences between frequencies.

Table 5: Comparison of frequencies identified from the general campaign and a reduced number of sensors.

As can be seen in Table 5, the results obtained by using the OSP method are actually similar to those obtained in the overall campaign. The relative differences between frequencies are always less than 2%, corroborating the use of the selected points to implement the SHM of this historical construction. With only four measurement points, the results obtained in terms of natural frequencies are really similar to those obtained from the general campaign, where a total of thirty-six points were monitored. Thus, the cost of maintaining a permanent monitoring system would be significantly reduced.

7. Conclusions

This paper presents a methodology to tailor a SHM of the E. Torroja bridge with a reduced number of sensors. This steel-composite structure presents singularities, mainly due to the fact that combines inverted steel arch trusses with a concrete deck. This geometric complexity along with the fact that was designed by the eminent Engineer Eduardo Torroja, make this structure of the utmost importance for the historical patrimony.

Initially, a concise historical description of the bridge was presented, focusing mainly on the geometric and structural aspects that make it such a singular work. Thereafter, the use of advanced techniques of structural analysis was essential to continue this study. In particular, OMA was used to experimentally determine the bridge modal properties from ambient vibration tests, in order to calibrate the FEM using genetic algorithms. The resulting updated FEM was subsequently used to prepare the structural health monitoring by using OSP techniques. Eight natural frequencies and their associated vibration modes were successfully identified, with MAC values ranging between 0.81 and 0.94 for the EFDD and SSI results.

Thanks to the identified natural frequencies, the FEM could be updated using two design variables. The adjustment was performed using in the finite element model of the bridge the effect of genetic algorithms as optimization technique. The dynamic response of the numerical model was successfully adjusted to the experimental results, with the frequency differences below 4% for the first eight vibration modes and obtaining MAC values between 0.82 and 0.96.

The updated FE model was then used to plan the SHM of the bridge by using OSP techniques. Specifically, the EFI method was used to determine the four optimal points to place the sensors.

The results demonstrate that with only four sensors, the resonant frequencies of the structure can be determined with less than a 2% error in comparison to the extensive monitoring with thirty-six measurement points.

In conslusion, ambient vibration tests, OMA, FEM updating and EFI technique have proven as valuable tools to devise monitoring schemes with a reduced number of sensors apt for long-term monitoring of the structural health of this kind of historical constructions.

Acknowledgements

The authors are pleased to acknowledge the Regional Government of Andalusia, for the support and the availability supplied during the experimental campaign. On the other hand, we cannot forget the help given by the researches of the investigation groups TEP-167 and TEP-245 of the Universities of Granada and Seville respectively. E. G-M was also supported by a FPU contract-fellowship from the Spanish Ministry of Education Ref: FPU13/04892.

BIBLIOGRAPHY

[1] T. Trker, A. Bayraktar, Structural safety assessment of bowstring type RC arch bridges using ambient vibration testing and finite element model calibration, Measurement 58 (2014) 33–45.

[2] W. Torres, J. L. Almazán, C. Sandoval, R. Boroschek, Operational modal analysis and FE model updating of the metropolitan cathedral of santiago, chile, Engineering Structures 143 (2017) 169–188.

[3] C. Pepi, M. Gioffrè, G. Comanducci, N. Cavalagli, A. Bonaca, F. Ubertini, Dynamic characterization of a severely damaged historic masonry bridge, Procedia Engineering 199 (2017) 3398–3403.

[4] B. Conde, L. F. Ramos, D. V. Oliveira, B. Riveiro, M. Solla, Structural assessment of masonry arch bridges by combination of non-destructive testing techniques and three-dimensional numerical modelling: Application to vilanova bridge, Engineering Structures 148 (2017) 621–638.

[5] C. Gentile, A. Saisi, Operational modal testing of historic structures at different levels of excitation, Construction and Building Materials 48 (2013) 1273–1285.

[6] A. C. Altunişik, A. Bayraktar, B. Sevim, F. Birinci, Vibration-based operational modal analysis of the mikron historic arch bridge after restoration, Civil Engineering and Environmental Systems 28 (3) (2011) 247–259.

[7] E. Torroja, Razón y ser de los tipos estructurales, Consejo Superior de Investigaciones Científicas, 2008.

[8] E. García-Macías, R. Castro-Triguero, R. Gallego, J. Carretero, Ambient vibration testing of historic steel-composite bridge, the e. torroja bridge, for structural identification and finite element model updating, in: Conference Proceedings of the Society for Experimental Mechanics Series, Springer International Publishing, 2015, pp. 147–155.

[9] S. Dassault Systemes, Abaqus/CAE 6.13 User's Guide (2015).

[10] J. L. S. Ramos, Damage identification on masonry structures based on vibration signatures, Ph.D. thesis, Universidade do Minho (2007).

[11] J. Rodrigues, Identificação modal estocastica, metodos de analise e aplicações em estruturas de engenharia civil., Ph.D. thesis, Engineering Faculty of University of Porto (2004).

[12] L. Ramos, L. Marques, P. Lourenço, G. D. Roeck, A. Campos-Costa, J. Roque, , Mechanical Systems and Signal Processing 24 (5) (2010) 1291–1305.

[13] S. V. Solutions, Artemis modal 5.0. User's Guide (2015).

[14] T. Wang, O. Celik, F. Catbas, L. Zhang, A frequency and spatial domain decomposition method for operational strain modal analysis and its application, Engineering Structures 114 (2016) 104–112.

[15] R. Brincker, L. Zhang, P. Andersen, Modal identification of output-only systems using frequency domain decomposition, Smart Materials and Structures 10 (3) (2001) 441–445.

[16] B. Peeters, G. D. Roeck, Reference-based stochastic subspace identification for output-only modal analysis, Mechanical Systems and Signal Processing 13 (6) (1999) 855–878.

[17] B. Peeters, G. D. Roeck, Stochastic system identification for operational modal analysis: A review, Journal of Dynamic Systems, Measurement, and Control 123 (4) (2001) 659.

[18] R. J. Allemang, D. L. Brown, A correlation coefficient for modal vector analysis, in: International Modal Analysis Conference, 1983.

[19] P. Brewick, A. Smyth, An investigation of the effects of traffic induced local dynamics on global damping estimates using operational modal analysis, Mechanical Systems and Signal Processing 41 (1-2) (2013) 433–453.
[20] P. Pachón, V. Compán, E. Rodríguez-Mayorga, A. Sáez, Control of structural intervention in the area of the roman theatre of cadiz (Spain) by using non-destructive techniques, Construction and Building Materials 101 (2015) 572–583.
[21] A. Teughels, Inverse modelling of civil engineering structures based on operational modal data, Ph.D. thesis, University of Leuven (2003).
[22] MathWorks, MATLAB R2015a. User's Guide (2015).
[23] R. C. Triguero, S. Murugan, R. Gallego, M. I. Friswell, Robustness of optimal sensor placement under parametric uncertainty, Mechanical Systems and Signal Processing 41 (1-2) (2013) 268–287.
[24] M. Meo, G. Zumpano, On the optimal sensor placement techniques for a bridge structure, Engineering Structures 27 (10) (2005) 1488–1497.
[25] D. Kammer, L. Yao, , Journal of Sound and Vibration 171 (1) (1994) 119–139.